P-ISSN 2586-9000
E-ISSN 2586-9027
Homepage : https://tci-thaijo.org/index.php/SciTechAsia
Science & Technology Asia
Vol.26 No.1 January - March 2021
Page: [189-198]
Original research article

Ophidascaris baylisi (Nematoda: Ascarididae): Scanning Electron Microscopic Study of the Adult Surface with Ultrastructure and Chemical Composition Analysis of Eggshells

Arin Ngamniyom[1,*] , Weerawich Wongroj[2], Kriangkrai Karnchaisri[3], Ruthairat Siriwattanarat[4]

[1]*Major in Environment, Faculty of Environmental Culture and Eco-tourism, Srinakharinwirot University, Bangkok 10110, Thailand*
[2]*Prasarnmit Elementary Demonstration School, Srinakharinwirot University, Bangkok 10110, Thailand*
[3]*College of Allied Health Sciences, Christian University, Bangkok 10400, Thailand*
[4]*Faculty of Science and Technology, Suan Sunandha Rajabhat University, Bangkok 10300, Thailand*

Received 23 September 2019; Received in revised form 5 June 2020
Accepted 11 August 2020; Available online 16 March 2021

ABSTRACT

The ascaridoid nematode *Ophidascaris* Baylis 1920 widely infests various species of snakes, including pythons. The aims of this study were to report the surface architecture of *Ophidascaris baylisi* gathered from Burmese pythons, using scanning electron microscopy, as well as to observe the ultrastructure and chemical composition of their eggshells using transmission electron microscopy and field emission scanning electron microscopy with energy dispersive X-Ray, respectively. In details of the surfaces, cephalic projections, body cuticle, single and double papillae, spicule, and egg pits were represented. The ultrastructure of the eggshells were composed of four layers: a uterine-like layer, vitelline layer, chitinous layer, and lipid layer. The eggshell surfaces were composed of C (48.17 ± 5.67% of total weight), O (23.10 ± 2.52), N (21.11 ± 2.68), S (1.39 ± 1.12), Na (1.20 ± 0.31), Ca (1.44 ± 0.74), P (2.12 ± 1.23), and Si (0.75 ± 0.12). Inside eggshells, C (50.30 ± 1.48), O (20.05 ± 1.96), N (19.60 ± 2.71), S (1.24 ± 0.22), Na (1.21 ± 0.41), Ca (1.01 ± 0.31), and P (6.59 ± 1.61) were detected, whereas Si was not. These data may be important in facilitating species identification and diagnosis, by using the microstructure, ultrastructure, and elemental composition of this nematode. This report raises concerns that there may be a zoonotic transmission of nematodes from pythons to humans or pets.

Keywords: *O. baylisi*; Python; Ultrastructure; FESEM-EDX

***Corresponding author:** arin@g.swu.ac.th
doi: 10.14456/scitechasia.2021.17

1. Introduction

Baylis (1921) described finding the ascaridoid *Ophidascaris*, belonging to the Ascarididae family, in host snakes. Since then, more than 10 species have been recognized in this genus [1-2]. Pythons are often infested by *Ophidascaris*, including *O. filaria* in *Python sebae* and *O. infundibulicola* and *O. baylisi* in *P. Reticulatus* (presently *Malayopython reticulatus*) and *P. curtus* [2-3]. Burmese pythons (*P. bivittatus*) are known to be some of the largest snakes native to Southeast Asia [4]. They are also a part of the local pet trade, like other species of python [5-6]. Therefore, this study aimed to investigate the surface morphology, some ultrastructure, elemental composition of eggshells, and preliminary molecular data of *O. baylisi* naturally infesting Burmese pythons. This report may provide important data to improve our knowledge of ascaridoid nematodes in pythons.

2. Materials and Methods

Ascaridoid nematodes were collected from the intestines of two Burmese pythons from a suburb of Bangkok in October 2018. These python intestines were given by local people who were living near an agricultural area, where pythons are regularly killed in order to protect farm animals and pets. Live nematodes were collected and washed with 0.9% normal saline. They were identified as *O. baylisi* according to the descriptions of *Ophidascaris* by Sprent [2, 7]. For analysis by field emission scanning electron microscopy with energy dispersive X-Ray (FESEM-EDX), nematodes were killed using 4% hot formaldehyde, fixed with 4% glutaraldehyde (for eggs and *O. baylisi*), prepared in 0.1 M phosphate buffer at 4 °C, re-fixed with 2% osmium tetroxide in 0.1M phosphate buffer at 25 °C, washed with distilled water, dehydrated using serial grade ethanol, and then dried by critical-point drying. Specimens were coated with Pt/Pd using a sputter coater, and the samples were viewed using an SEM-HITACHI SU-8010 with an acceleration of 5.0 or 15.0 kV. X-ray elemental analysis was performed using an XFlash 6 detector under high-vacuum mode, and the accelerating voltage was set to 20 kV for EDX images, with 60 s as the determined counting time. The insides of eggshells were investigated using the element profiles from cracked eggs. In TEM analysis, ascaridoid eggs were prepared in the same way as the SEM protocol. After dehydration, specimens were moved into propylene oxide and epoxy resins (Araldite-502) for infiltration, embedded in the resin, and incubated at 45 °C for 24 h and 60 °C for 24 h. They were sectioned as thin films, stained with uranyl acetate for 30 min, and re-stained with lead citrate for 35 min on carbon coated Cu grids. Results were obtained using a JEOL JEM-1400 series at 100 kV.

Genomic DNA was extracted from living male and female specimens using a DNeasy Tissue Kit (Qiagen). Primers paired for cytochrome c oxidase subunit I (CO1) (ggYACCCCTCCWTCWTTgTCKTT and CACCAgTAggMACAGCAATAACC) were used for gene amplification with Taq DNA polymerase. The PCR protocol was performed as follows: initial denaturation at 95 °C for 5 min, followed by 30 cycles of denaturation at 94 °C for 30 s, annealing at 55 °C for 40 s, extension at 72 °C for 90 s, and a final extension for 10 min. PCR products were purified by electrophoresis using the QIAquick Gel Extraction Kit (Qiagen). DNA sequencing analysis was performed by the Macrogen DNA Sequencing Service, Korea. The CO1 partial sequences were deposited into GenBank with the accession number MT450841. Sequences were aligned with the Clustal Omega multiple sequence alignment program; the neighbor joining (NJ), minimum evolution (ME), maximum likelihood (ML), and unweighted pair group method with arithmetic mean (UGMA) phylogenetic trees were made by MEGA 6.

Animal experiments were conducted following all national and institutional guidelines for Animal Care and Use by the Institute of Animals for Scientific Purpose Development (IAD) National Research Council of Thailand (NRCT) following a permission license (U1-04855-2559).

3. Results and Discussion

The present study reported on *O. baylisi* found in the intestines of Burmese pythons. *Ophidascaris baylisi* were collected from intestines of two pythons. Twenty-seven nematodes (10 males and 17 females) were found in python number 1, and 42 nematodes (14 males, 23 females, and 5 unknown sex) were found in number 2. The prevalence (%) and mean density were 100 and 48 respectively. The body size of males (n = 6, 88.2 ± 20.9 mm, range of 67–121) was shorter than that of the female nematodes (n = 6, 118.3 ± 30.3 mm, range of 93–162). According to the reports of Sprent [2, 7], the reticulated python (*M. reticulatus*) is a host of *O. baylisi*, and this nematode can be classified under the filaria group. Reticulated pythons can be found throughout Thailand, and their distribution overlaps with that of the Burmese python, in northern and central Thailand [8, 9]. It was confirmed that *O. baylisi* could be found among the related species of pythons and may be associated with the ecological habitat.

With regards to microstructure, the tooth of the *O. baylisi* lanceolate was found to be stout with smooth surfaces (Figs. 1A and 1B). On the lateral lip, a single papilla could be found centered and separate the amphid from the double papillae. Amphids (n = 6, 7.1 ± 1.2 μm in diameter, range of 5.9–8.4) were observed to be ovoid and positioned level with the single papilla (n = 4, 9.73 ± 1.6 μm, range of 7.6–11.3). Double papillae (n = 6, 23.5 ± 2.6 μm in length, range of 20.2–26.1, and 12.8 ± 2.1 μm in width, range of 10.9–15.22) were oblong and large, but single papillae were round and small (Fig. 1C). Interlabia were shaped like equilateral triangles with smooth surfaces. Grooves between the interlabium and lateral lip were deep (Fig. 1C). In the dorsal lips, one pair of double papillae was observed at either side (Fig. 1D). The micrographs of *O. baylisi* in ventral and dorsolateral views corresponded to the morphologies of the filaria group (*O. moreliae*, *O. infundibulicola*, and *O. Baylisi*) according to the descriptions of Sprent [7]. The interlabial feature of *O. baylisi* in this study showed little difference to those described in *O. moreliae* and *O. infundibulicola* [7] and were quite different from those in the arndti group (*O. arndti* and *O. sicki*), obconica group (*O. obconica*, *O. trichuriformis*, *O. ashi*, *O. mombasica*, and *O. excavata*), radiosa group (*O. radiosa*) [2], and najae group (*O. wangi* and *O. najae*) [10]. The interlabial feature of *O. baylisi* was triangular in shape, same as *O. moreliae and O. infundibulicola*, but the interlabial aspects of *O. baylisi* was more slender than those of *O. moreliae* and *O. infundibulicola.* The teeth of *O. baylisi* was similar in shape to *O. wangi* [10] and *O. excavate* [11]. However, they were different from *O. najae* [10] and *O. trichuriformis* [2]. Therefore, these data may support the consideration of anterior characteristics of *O. baylisi* when performing identification.

From the anterior aspect to the beginning of the midsection, annuli were alternated by narrow furrows (Fig. 2A). In the midsection, annular furrows on the surface were not predominant, unlike the anterior body (Fig. 2B). The surface appeared to be a corrugated shape for both males and females. In females, the vulva (n = 6, 73.4 ± 4.6 μm in length, range of 68.4–79.2, and 18.3 ± 3.5 μm in width, range of 14.5–22.24) displayed strong musculature, and annular furrows surrounding the outside of the vulvar opening. The inside of the opening of the vulva was grooved but was not long or in a network (Fig. 2C–D). In the posterior part, numerous single papillae (n = 80, 9.0 ± 3.0 μm in diameter, range of 4.8–

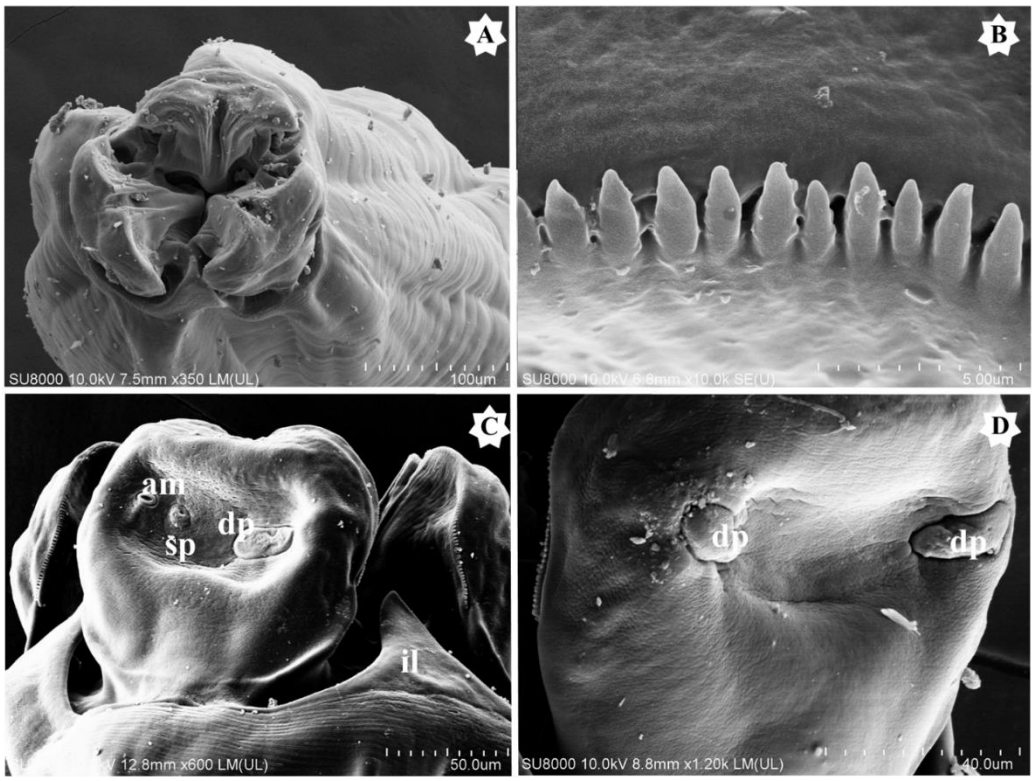

Fig. 1. Scanning electron micrographs of *O. baylisi*. Cephalic end and apical view of nematode (A), tooth (B), magnified image of ventrolateral lip (C), dorsoventral-lateral lip (D). Abbreviations: am, amphid; dp, double papillae; il, interlabium; sp, single papilla.

14. 2) lined the ventrolateral aspect of the body on the posterior aspect (Figs. 3A, 4B). The cloaca opened in a crescent-like shape and had a rough surface at the anterior end (Fig. 2B). Two pairs of double papillae (n = 8, 15.1 ± 1.8 μm in diameter, range of 12.3–17.0) were embedded lateral to the paracloacal opening in both sexes (Figs. 3D, 4C). In the post- cloacal region, single papillae (n = 20, 9.1 ± 2.1 μm in diameter, range of 5.9–12.1) were similar in shape to the single papillae found in the paracloacal region (Figs. 3A, 3C, 4A). In males, the spicule projection was short and stout. The spicule surface was a bit rough and was predominated by longitudinal lines (Fig. 4A, B). Transverse lines were found in the paracloacal double papillae of males (Fig. 4C). In eggs, they are nearly spherical. Many large pits were found, deep and separated by narrow ridges (Fig. 4D and 4E). The pairs of paracloacal double papilla of *O. baylisi* that were seen under SEM micrographs corresponded to the morphological description of a filaria group [7] and were similar to the microstructure of *O. wangi* [10], *O. radiosa,* and *O. mombasica* [2]. However, the pairs of paracloacal double papilla of *O. baylisi* were different from those of *O. najae* and *O. excavate*, which had a paracloacal single or double papilla on each side of the lateral cloaca [10, 11]. This SEM data confirmed the morphology of the paracloacal papilla of *O. baylisi* and may be helpful in the identification of *Ophidascaris*. However, the morphology of the paracloacal papilla of *O. baylisi* was incongruent to some in the *Ophidascaris* group. The egg surfaces (n = 50) of *O. baylisi* had large, deep pits that were similar to those found on the eggs of *O.*

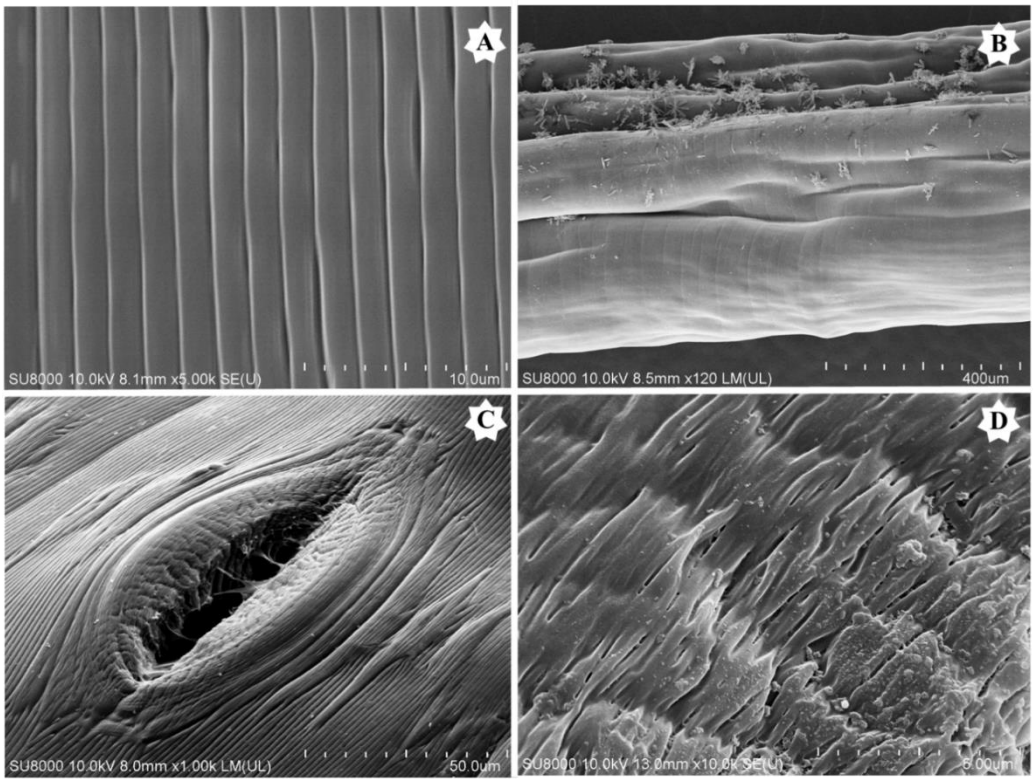

Fig. 2. Scanning electron micrographs of *O. baylisi*. Annuli alternated by narrow furrows on anterior part (A), surface of the beginning of the middle body (B), vulva (C), magnified image of vulva (D).

baylisi, and were different from those of *O. moreliae* and *O. infundibulicola* seen under a light microscope, as described by Sprent's report [2]. It was also confirmed by micrographs that egg morphologies were specific for each species in the filaria group.

In terms of ultrastructure (n = 50), the eggshell consisted of 4 layers: a uterine-like layer, vitelline layer, chitinous layer, and lipid layer. The uterine-like layer is covered by a coating of densely staining material. The vitelline layer is thin. Electron dense-like granules were found in both the vitelline layer and chitinous layer. The lipid layer, with electron dense lines, is closed to the undeveloped embryonic content and contains lipid droplets and granules (Figs. 5A–B). In ascaridoid nematodes, the layers of eggshells of *O. baylisi* were similar to those of *Ascaris lumbricoides* [12-13]. However, in the eggshells of *O. baylisi*, the electron intensity of the chitinous layer near the vitelline layer was darker than the part of the layer near the lipid layer (Figs. 5C, D).

According to FESEM-EDX analysis, eggshell surfaces (n = 5) were composed of C (48.17 ± 5.67% of total weight), O (23.10 ± 2.52), N (21.11 ± 2.68), S (1.39 ± 1.12), Na (1.20 ± 0.31), Ca (1.44 ± 0.74), P (2.12 ± 1.23), and Si (0.75 ± 0.12). Elemental composition inside eggshell surfaces was comprised of C (50.30 ± 1.48), O (20.05 ± 1.96), N (19.60 ± 2.71), S (1.24 ± 0.22), Na (1.21 ± 0.41), Ca (1.01 ± 0.31), and P (6.59 ± 1.61). In contrast, Si was undetectable (Fig. 5E–G). According to a study by Clarke et al. [14], Ca, Al, Cu, Mg, Si, Fe, and Mn were detected in the eggshell ash of *Heterodera rostochiensis* using spectrographic analysis. The elemental composition of eggshells of *O.*

baylisi was similar to that of *H. rostochiensis* in terms of Ca and Si content, but did not include Al, Mg, or traces of other elements. It was suggested that the presence of those elements might be required for the biochemical deposition or maintenance of eggshell structure of *O. baylisi*

Two *O. baylisi* were monophyletic with the related species of genus *Ophidascaris* from the nucleotide databases of The National Center for Biotechnology Information (NCBI) and separated from *Ortleppascaris sinensis*, *Toxascaris leonine* and *Ascaris suum*. *Ophidascaris baylisi* were clearly isolated from *Microdevario nana* (teleost) that were used as an outgroup (Fig. 6). This molecular result confirmed *Ophidascaris*, based on the nucleotide sequences of the mitochondrial COI gene from NCBI [15]. The provided nucleotide sequences of *O. baylisi* may be useful for DNA barcoding, in this species.

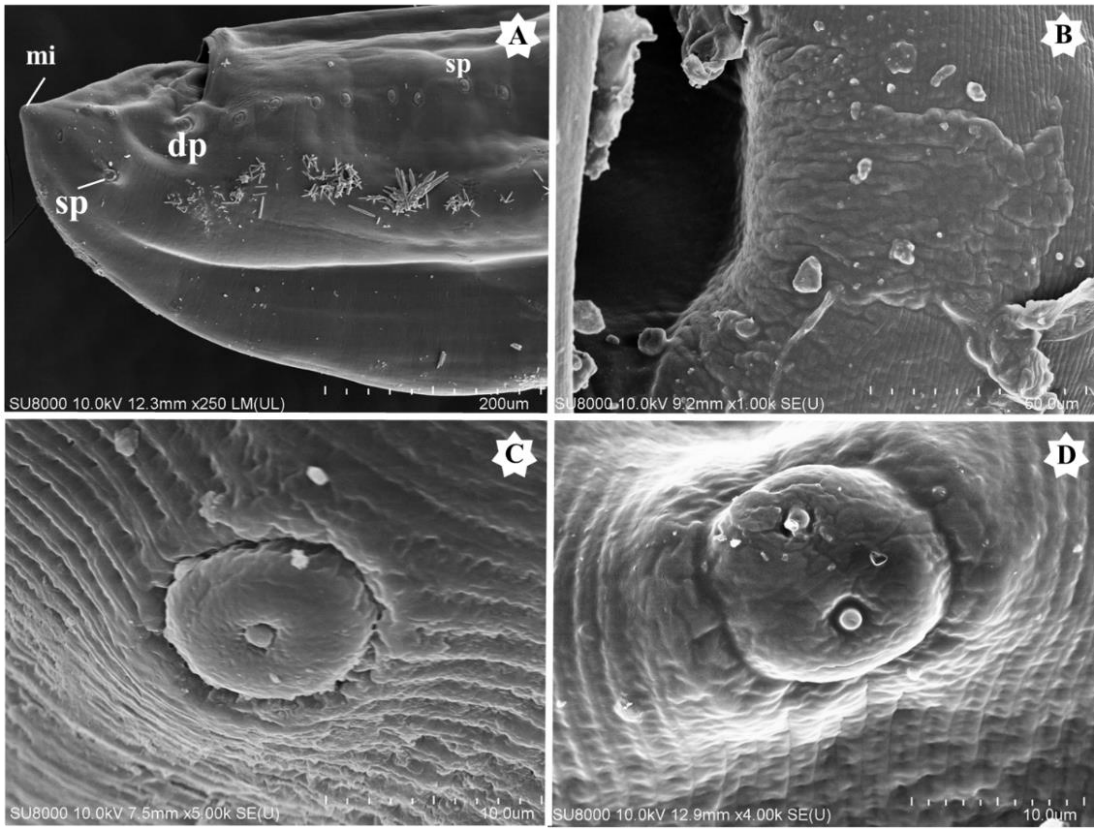

Fig. 3. Scanning electron micrographs of *O. baylisi*. Posterior end of female (A), cloaca of female (B), postcloacal ventrolateral single papilla (C), paracloacal double papilla of female (D). Abbreviations: dp, double papillae; il, interlabium; mi, mucron; sp, single papilla; spi, spicule.

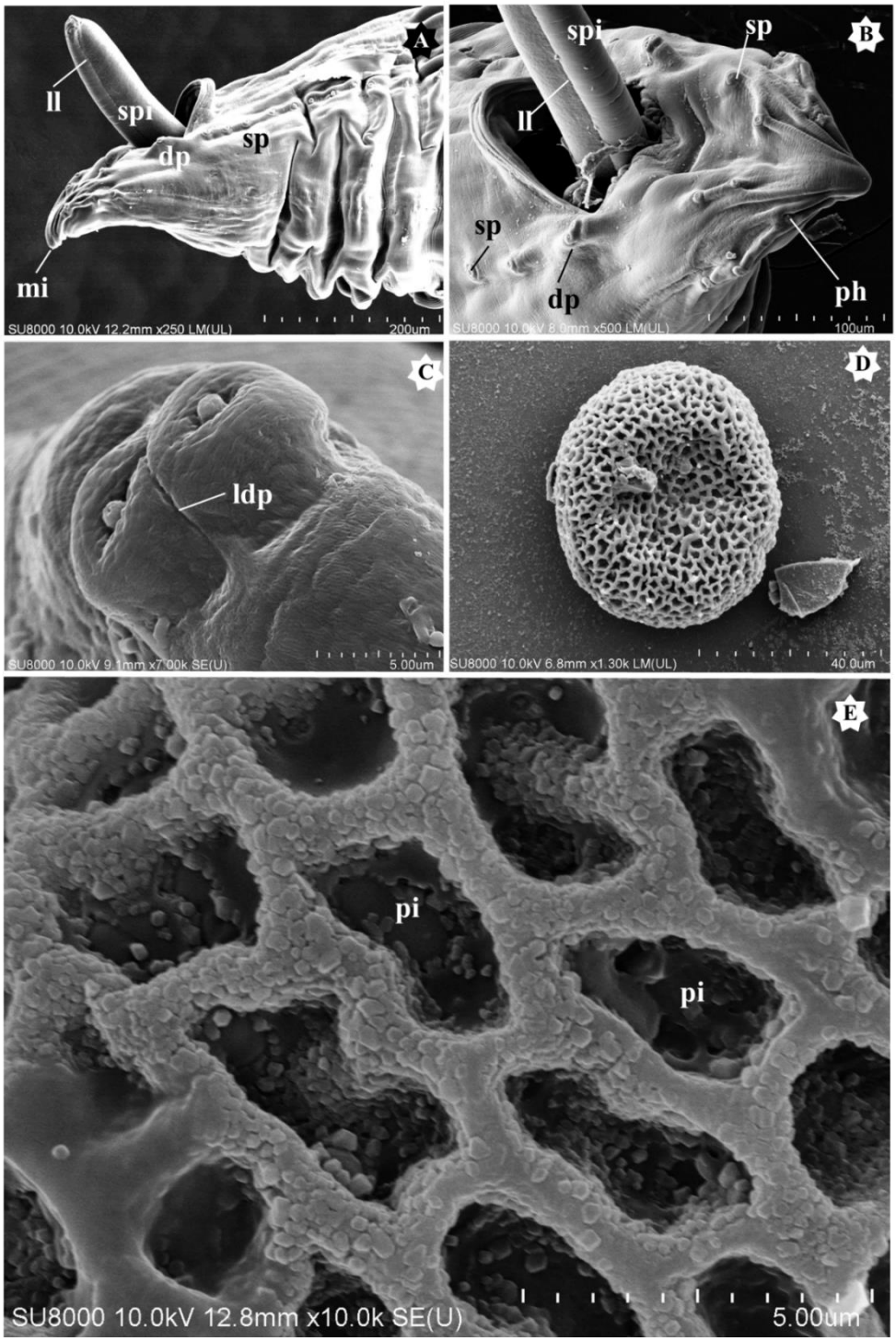

Fig. 4. Scanning electron micrographs of *O. baylisi*. Posterior end of male (A), cloacal region of male (B), paracloacal double papilla of male (C), eggshell (D), high magnification image of eggshell (E). Abbreviations: dp, double papillae; mi, mucron; ldp, transversal line of double papillae; ll, longitudinal line of spicule; pi, pit; ph, phasmid; sp, single papilla; spi, spicule.

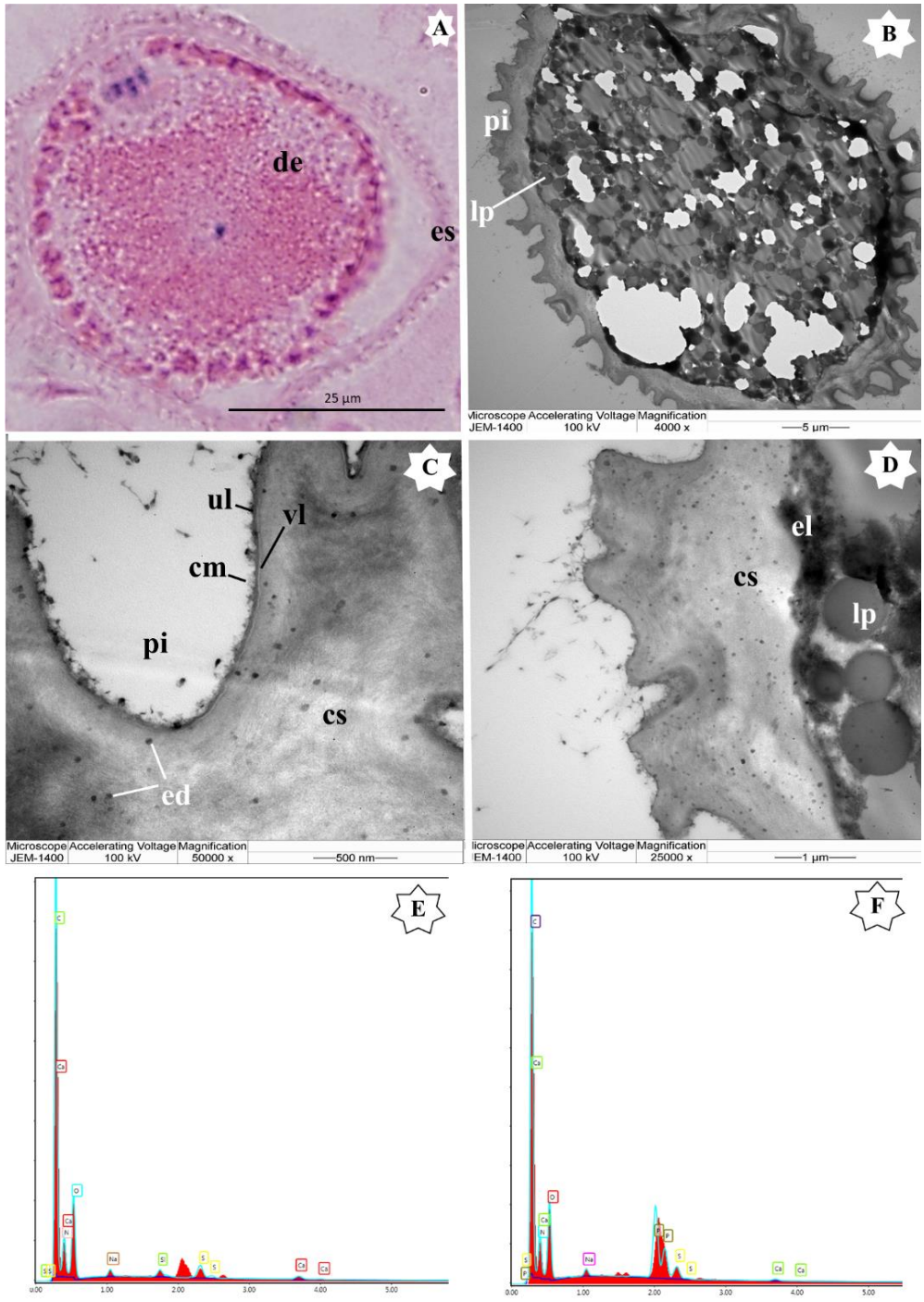

Fig. 5. Histological view of egg by H&E staining (A), ultrastructure egg of *O. baylisi* (B), high magnification image of egg shell (C, D), X-Ray spectroscopy displayed elemental analysis of surface (F) of eggshell, inside (F) of cracked egg shell and percentage of weight of elements (I). Abbreviations: cm, coating of densely staining material; cs, chitinous layer; ed, electron dense-like granules; el, electron dense line; es, egg shell; de, embryonic material; lp, lipid droplet; pi, pit; ul, uterine-like layer; vi, vitelline layer.

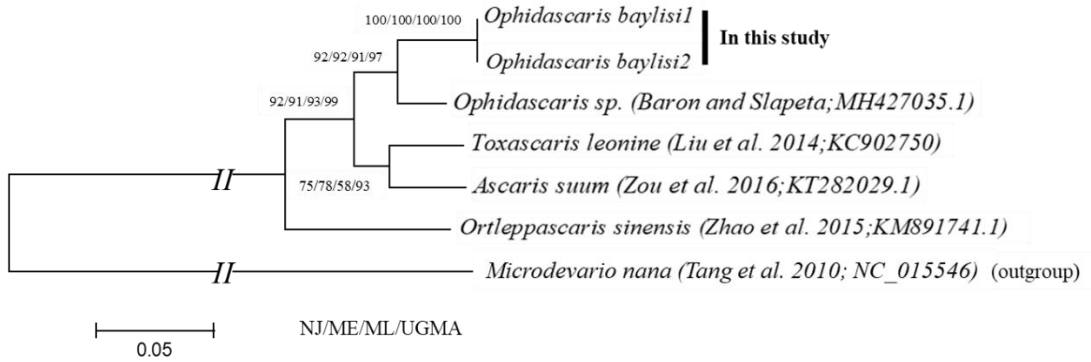

Fig. 6. Molecular phylogenetic tree of *O. baylisi* and other species based on COI gene sequence, by the methods of neighbor joining (NJ), minimum evolution (ME), maximum likelihood (ML), and unweighted pair group method with arithmetic mean (UGMA) with 1000 replications.

4. Conclusion

In this study, we displayed the surface ultra- architecture and elemental profile of eggshells of *O. baylisi*. Some structures might provide further insights useful in *Ophidascaris* identification, and increase the knowledge on the chemical compositions of their species' eggshells. The micro-and ultra-structure exhibit some species- specific characteristics and elemental composition. This report raises concerns that there may be a zoonotic transmission of nematodes from pythons to humans or pets.

References

[1] Sprent JFA. Ascaridoid nematodes of amphibians and reptiles: *Ophidascaris* Baylis, 1920. Syst Parasitol 1988; 11: 165.

[2] Baylis HA. On the classification of the Ascaridae. II. The Polydelphis group; with some account of other ascarids parasitic in snakes. Parasitol 1921; 12: 411–26.

[3] Elbihari S, Hussein MF. *Ophidascaris filaria* (Dujardin 1845) from the African rock python, Python sebae, in the Sudan, with a note on associated gastric lesions. J Wildl Dis 1973; 9(2): 171–3.

[4] Barker DG, Barker TM. The distribution of the Burmese python, *Python molurus bivittatus*. Bull Chicago Herpetol Soc 2008; 43(3) : 33–8.

[5] Mariana A, Vellayan S, Halimaton I, Ho TM. Acariasis on pet Burmese python, *Python molurus bivittatus* in Malaysia. Asian Pac J Trop Med 2011;4(3):227-8.

[6] Fonseca É, Solé M, Rödder D, de Marco P. Pet snakes illegally marketed in Brazil: Climatic viability and establishment risk. PLoS One 2017; 12(8): e0183143.

[7] Sprent, JFA. Studies on ascaridoid nematodes in pythons: speciation of *Ophidascaris* in the Oriental and regions. Parasitol 1969; 59(4) : 937–59.

[8] McDiarmid RW, Campbell JA, Touré TA. Snake Species of the World: A Taxonomic and Geographic Reference, Volume 1, Washington, DC, Herpetologists' League; 1999, 511 pp.

[9] Stuart B, Nguyen TQ, Thy N, Grismer L, Chan-Ard T, Iskandar D, Golynsky

E, Lau MWN. *Python bivittatus*. The IUCN Red List of Threatened Species. 2012; e.T193451A2237271.

[10] Li L, Guo YN, Li J, Zhang LP. *Ophidascaris wangi* sp. n. and *O. najae* (Gedoelst, 1916) (Ascaridida: Ascaridoidea) from snakes in China. Folia Parasitol (Praha) 2014; 61(6): 571–80.

[11] Li L, Zhao WT, Chen HX, Guo YN, Zhang LP. Morphological study of *Ophidascaris excavata* Hsü & Hoeppli, 1931 (Ascaridida: Ascarididae) from *Gloydius brevicaudus* (Stejneger) (Reptilia: Viperidae). Syst Parasitol 2016; 93(1): 69 –75.

[12] Rogers RA. A study of eggs of *Ascaris lumbricoides* var. suum with the electron microscope. J Parasitol 1956; 42(2): 97 –108.

[13] Lýsek H, Malínský J, Janisch R. Ultrastructure of eggs of *Ascaris lumbricoides* Linnaeus, 1758. I. Egg-shells. Folia Parasitol (Praha) 1985; 32(4): 381 –4.

[14] Clarke AJ, Cox PM, Shepherd AM. The chemical composition of the egg shells of the potato cyst- nematode, *Heterodera rostochiensis* Woll. Biochem J 1967; 104(3): 1056 –60.

[15] Sayers EW, Cavanaugh M, Clark K, Ostell J, Pruitt KD, Karsch-Mizrachi I. GenBank. Nucleic Acids Res. 2019; 47(D1):D94–9